geosciences

MDPI

Article

Census-Based Typological Damage Fragility Curves and Seismic Risk Scenarios for Unreinforced Masonry Buildings

Maria Zucconi [1,*] and Luigi Sorrentino [2]

[1] Department of Engineering, University Niccolò Cusano, Via Don Carlo Gnocchi 3, 00166 Roma, Italy
[2] Department of Structural and Geotechnical Engineering, Sapienza—University of Rome, Via Antonio Gramsci 53, 00197 Roma, Italy; luigi.sorrentino@uniroma1.it
* Correspondence: maria.zucconi@unicusano.it

Abstract: Seismic risk assessment has become a crucial issue for optimal management of economic resources allocated to mitigation. For this purpose, in the last decades, several research activities were aimed to update hazard, exposure, and vulnerability models that contribute to seismic risk assessment. From this perspective, the present work focuses on developing new empirical damage fragility curves for census-based typological unreinforced masonry buildings. In particular, damage data observed after the 2009 L'Aquila earthquake, Italy, related to almost 57,000 residential buildings, were used to calibrate the fragility functions. These data were complemented with the census data with the aim of obtaining an accurate estimation of the number of undamaged buildings. Damage fragility curves were identified for typological building classes, defined considering parameters present in both post-earthquake observations and census data with the aim of extending the results to the whole national territory. Six typological classes were defined considering the categories of the construction timespan and of the state of repair parameters. Then, a further distinction of the typological classes considering the number of stories parameter was included where relevant. The fragility curves were defined as a function of peak ground acceleration for five damage states, defined according to the European macroseismic scale. The results confirmed that older buildings are more vulnerable than newer ones and highlighted the crucial role of the state of repair on the damage fragility curves. Finally, the new set of damage fragility functions was uploaded in the Italian Risk Maps information technology platform, used by the Civil Protection Department for risk evaluation, as an exemplification of the potential application of the fragility curves.

Keywords: state of repair; construction timespan; number of stories; damage states; typological classes; simulation of uninspected buildings; damage seismic risk map; maximum likelihood estimation; 2009 L'Aquila earthquake; AeDES form

Citation: Zucconi, M.; Sorrentino, L. Census-Based Typological Damage Fragility Curves and Seismic Risk Scenarios for Unreinforced Masonry Buildings. *Geosciences* **2022**, *12*, 45. https://doi.org/10.3390/geosciences12010045

Academic Editors: Giuseppe Lacidogna, Rosa Nappi and Jesus Martinez-Frias

Received: 13 December 2021
Accepted: 10 January 2022
Published: 17 January 2022

1. Introduction

In the last few decades, different significant earthquakes of medium magnitude occurred in Italy, underlining the great vulnerability of existing buildings stock [1–3]. As a consequence of the occurred seismic events, relevant economic losses [4–7] and a high number of casualties were registered, pointing out the importance of the prevention activities (e.g., [8,9]) and the proper management of funds by the public administrations [10–12]. In light of the above, the Civil Protection Department has a key role in funds allocation in Italy. In the last years, many projects received public financial support intending to update the 2018 Italian National Seismic Risk Assessment [13,14].

The Italian Risk Maps information technology platform (IRMA) [14,15], used by the Civil Protection Department for the seismic risk assessment, was updated in the last years thanks to the contribution of many research groups that focused on the different aspects involved in risk evaluation, such as hazard, exposure, and vulnerability.

Among the different vulnerability models available in the literature, empirical fragility curves, based on observed damage, are largely widespread in Italy thanks to the recent publication of the data collected after the most relevant Italian earthquakes occurred in the last fifty years by the Civil Protection department throughout the DaDO (Observed Damage Database) platform [16,17]. Empirical methods were developed since the 1970s (e.g., [18]) and, in the last years, many models were developed for both reinforced concrete buildings [19–23] and unreinforced masonry buildings (URM) [1,24–30]

The empirical models require to define different aspects that can influence their effectiveness, among them the most relevant: (i) the selection of the intensity measure; (ii) the classification of the typological classes; (iii) the definition of a global damage index; and (iv) the probabilistic distribution adopted to fit the observed data.

Macroseismic intensity and peak ground acceleration (*PGA*) are the most-frequently selected intensity measures [20,28,31,32]. The *PGA* is the most common choice since it is an instrumental measure, different from the macroseismic intensity that is a conventional estimation of ground shaking severity based on observed effects in a limited area [33].

The empirical models are defined for typological building classes [2,18,21,34] or considering a vulnerability index as a function of different structural parameters [25–27,35,36]. A high number of parameters leads to a more accurate estimation, but the information required are not always simple to get for a large-scale vulnerability assessment (e.g., [25,36]). Contrarily, simplified typological classes, based on a reduced number of parameters, e.g., the timespan of construction and the number of stories (e.g., [20,21]), lead to more approximate results, but the information can easily be collected for the whole national territory from the census data [37]. In fact, census data was used to derive fragility curves or regional loss estimation in different countries [38,39].

Then, the definition of a building damage state is a relevant issue for each empirical method. Different research groups proposed specific procedures to retrieve the damage suffered from the structure during an earthquake. In particular, the Italian AeDES form describes the damage level considering both severity and extension. The first parameter includes four severity categories: D0, no damage; D1, slight damage; D2–D3, medium-severe damage; and D4–D5, very heavy damage or collapse. The second parameter is defined as a fraction between the damaged surface and the total surface of the structural element. Different structural components are considered in the evaluation, including vertical structures, horizontal structures, roof, stairs, infill, and partitions. Numerous proposals are available in the literature to define the building damage state starting from the damage collected with the Italian AeDES form. Many authors consider only the damage suffered by the vertical structures [1,2,40,41]; Rota et al. [34] define the building damage state as the most severe damage level between vertical structures, horizontal structures, and roof; other authors account for the full combination of damage suffered by all components [28,42,43].

Finally, the choice of the probabilistic distribution adopted to fit the observed damage data, as well as the method selected to estimate the distribution parameters, can influence the shape of the fragility curves. Among them, the distributions most frequently employed for the empirical methods are the log-normal and the exponential ones, while the most widely used methods to estimate the distribution parameters are the maximum likelihood estimation method and the method of moments (e.g., [44,45]).

All empirical methods aim to estimate structural damage with the final goal to assess the seismic risk and to estimate repair costs. Alternative methods consider the usability [46], i.e., the ability of a building to be occupiable after a seismic event [1,27,47], instead of the damage. In fact, in Italy, after the 2009 L'Aquila earthquake, a criterion for allocating economic resources was based on usability assessment [10,48,49]. In this context, different authors correlated the usability outcome to the structural damage [1] or to structural features [50]. Differently from previous authors, Zucconi et al. [25,27,47,51] proposed an empirical model for the probabilistic assessment of the usability outcomes.

In this paper, a new set of empirical fragility curves is derived starting from the damage observed after the 2009 L'Aquila earthquake. The typological building classes were defined considering the information available in both damage and census databases with the aim to use the fragility curves to derive damage scenarios in different areas of the national territory. The structural features considered for the definition of the classes are the construction timespan and the state of repair. The last parameters proved to be the most significant for the fragility curves estimation. Moreover, the number of stories parameter was considered only where it was relevant. The selected intensity-measure was the *PGA* and the damage state was defined accounting for different structural components, according to Zucconi et al. [28]. Furthermore, the initial database of about 57,000 URM buildings was complemented with the census database [37], generating uninspected buildings with a Monte Carlo simulation, obtaining a final database of about 308,000 items. Finally, fragility curves were used to simulate damage risk maps within the IRMA platform for all the municipalities of the Abruzzo region.

2. L'Aquila Earthquake: Damage Database and Seismic Input

On 6 April 2009, the Abruzzo region was struck by a M_W 6.3 earthquake, with the epicenter located in the city of L'Aquila that was seriously damaged. Moreover, approximately 125 municipalities were involved by the seismic event, with an intensity measure ranging from V to IX grade of Mercalli-Cancani-Sieberg macroseismic scale (I_{MCS}).

After the earthquake, approximately 75,000 buildings were inspected within a survey coordinated by the Italian National Civil Protection Department, with the aim to collect geometrical, structural, damage information and tag the constructions in terms of usability. The inspection data were recorded in the Italian AeDES Form "Level 1 Form for Post-Earthquake Damage and Usability Assessment and Emergency Countermeasures in Ordinary Buildings" [52].

A subset of masonry buildings is selected from the original database for the following elaborations. In particular, forms are discarded if:

- The vertical structure is unknown or made of reinforced concrete or steel;
- The structure is not described in terms of quality of masonry, type of horizontal structure, presence of tie rods or tie beams;
- Footprint area is not reported;
- Damage fields are not filled in;
- Damage level and usability outcome are inconsistent (e.g., heavy damage associated with usability or no damage associated with an unusable building).

The remaining buildings amount to 58,365 belonging to 477 settlements, located in 125 municipalities (Figure 1). A description of the database, in terms of building features and performance, can be found in Zucconi et al. [27,47].

To take into account the actual total number of buildings present in the studied area, the subset is increased with an estimation of the undamaged buildings not inspected after the earthquake. In general, the buildings are inspected systematically only in the epicentral area, or near field, while further away from there, the alternatively-called far field, the inspection takes place only after an owner's request and, generally, the stakeholder is inclined to request an official inspection only if the building is damaged. The number of buildings to be added is estimated according to a methodology proposed by Zucconi et al. [47], based on the comparison between the number of buildings present in the AeDES database with that present in the census [37]. With additional undamaged buildings generated with a Monte Carlo simulation, the final analyzed database includes more than 375,000 items and avoids an overestimation of damage occurrence.

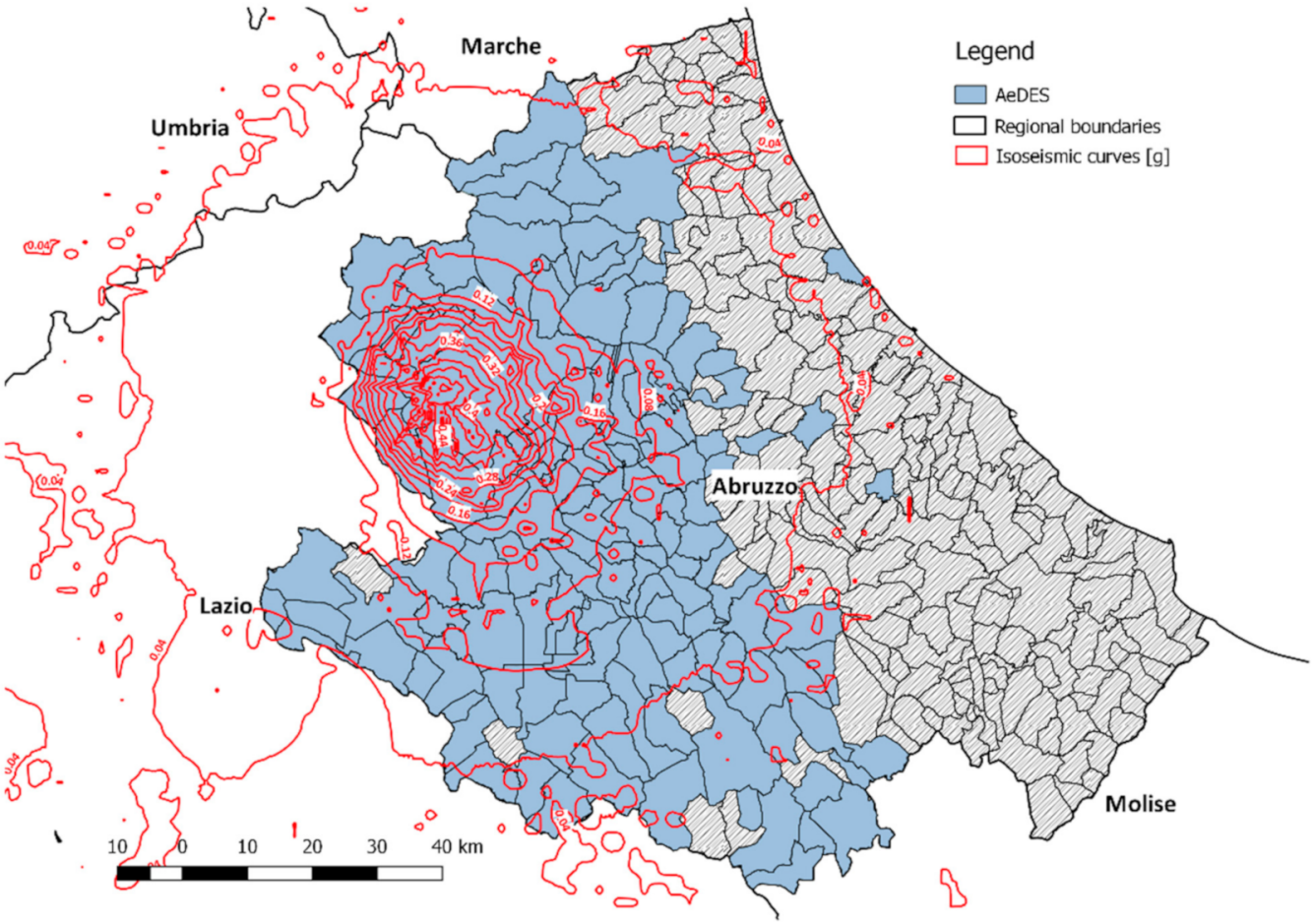

Figure 1. Abruzzo municipality boundaries and AeDES database coverage, superimposed on *PGA* shakemap. (Shakemap base from http://shakemap.rm.ingv.it/shake/1895389/products.html, accessed on 1 June 2021).

For the development of damage fragility curves, selecting a representative intensity measure to be assigned to each building in the database is necessary. Several intensity measures 9e.g., macroseismic intensity, *PGA*, peak ground velocity, and spectral acceleration for a given period of vibration) are common in the fragility-curves literature.

The macroseismic intensity was largely used in the past decades since it is applicable to historical seismicity and whenever the density of instrumentation is inadequate. Nevertheless, the macroseismic intensity is attributed conventionally and based on building performance, hence suffering to a varying extent from the building portfolio affected by the shaking. Moreover, hazard studies in terms of macroseismic intensity are not systematically available, making the preventive use of this intensity measure not straightforward. Conversely, ground motion intensity measures are structure-independent and available in post-event shakemaps [53]. Among them, *PGA* is usually the most popular intensity measure since it available in most hazard studies. Additionally, *PGA* is the intensity measure chosen by the Italian National Civil Protection Department for seismic damage scenarios and risk analyses [17]. Therefore, in the following, the *PGA* is assumed for deriving fragility curves.

PGA data were made available by the Italian National Institute of Geophysics and Volcanology in terms of shakemaps related to earthquakes since 2008. In particular, raw data related to the shakemaps of the 2009 L'Aquila earthquake [54] (http://shakemap.rm.ingv.it/shake/1895389/products.html, accessed on 1 June 2021) are considered for the following analyses. The shakemap *PGA* values vary between 0.02 and 0.48 g, with

a step of 0.04 g (Figure 1). These values are herein regrouped in bins, with a 0.10 g step, and the central value of each bin is chosen as the categorical value of the bin. Limited exceptions are considered for the first and the last bins, as shown in Table 1. A smaller step is considered in the first bin, while in the last bin, the categorical value is selected to be close to the mean of available data. Bins with a step of 0.05 g were tested without getting any significant improvement in the results. The categorical values of Table 1 were assigned to each building present in the database as a function of its location on the map.

Table 1. Peak ground acceleration (*PGA*) bins, categorical values, number of buildings in AeDES database, and increased (AeDES complemented with census) database.

Bin [g]	Category [g]	AeDES	Increased Database
<0.05	0.025	17,295	312,499
0.05 to <0.15	0.10	12,638	35,903
0.15 to <0.25	0.20	4957	4957
0.25 to <0.35	0.30	7073	7073
≥0.35	0.40	14,621	14,621
Total		56,584	375,053

3. Italian Census Database and Typological Building Classes

The Italian statistic institute takes care of the census survey of buildings and population over the whole national territory, collecting data that constitute relevant support for the decision-making of the national or local institutes. Census data became an important support to overcome the limitations of the AeDES damage data available only for the areas affected by past earthquakes.

The census database provides information about the main characteristics of the residential buildings, such as: structural material (URM, reinforced concrete, steel, mixed structure, etc.); construction timespan; number of stories above ground; number of underground stories, number of stairs; state of repair; presence of adjacent buildings; and number of dwellings.

Census data are collected based on a rapid visual screening of the building from the outside and on other administrative information available to public bodies. Contrarily, the AeDES data require a more accurate inspection and an internal visit of the structure unless damage is so extensive that risk to life and limb is too high. It is relevant to observe that the definition of the building is not exactly the same in the two surveys: in census form, the use is the main parameter to define a single building so that different structural units can be regrouped, while in AeDES form, the "building" is identified considering a single structural unit.

The typological building classes introduced in the following were defined considering the information available in both forms, with the aim to use the results to simulate damage scenarios in different localities, municipalities, or regions belonging to the Italian territory for which only census data are available. Contrarily, if only the more refined 2009 L'Aquila earthquake data are used to define the typological building classes. The results should be limited to the Abruzzo region and could not be used elsewhere.

With this purpose two-building characteristics available on both databases were selected: construction timespan and state of repair.

The definition of construction timespan is unique for both databases, differently from the state of repair that in census database is defined evaluating the general condition of the building, assessing the state of plaster, window fixtures, vertical structures, and roof. Then, four possible categories can be defined as follows:

- Excellent, if all construction elements present no damage;
- Good, if only plaster is deteriorated;
- Mean, if plaster and window fixtures are deteriorated, vertical structures are damaged but not the roof;

- Poor, if also the roof is damaged.

In the AeDES database, state of repair is not directly present but pre-existing damage to structural elements is reported. The damage scale defines four categories: D0, no damage; D1, negligible to slight damage; D2–D3, moderate to heavy damage; and D4–D5, very heavy damage to collapse. Then, three extension categories (<1/3,1/3–2/3, >2/3 of building surfaces) are defined for the damage scale.

An association between AeDES pre-existing damage and census state of repair is required to combine the information of the two databases. First of all, the four census categories were regrouped in two, R1 for Excellent and Good, and R2 for Mean and Poor state of repair. This choice is based on the fact that only the last two categories are related to structural damage. Then, R1 was associated with pre-existing damage classification D0 and D1 with an extension less than 1/3, and R2 with all other damage classifications. This association allows one to obtain a similar percentage distribution of buildings in the two databases. The census distribution was adopted for the Monte Carlo simulation.

For the construction timespan parameter three categories were defined: <1919, 1919–1961, >1961 [47], identified considering the main changes in Italian standards for URM constructions.

Combining the categories of the two selected parameters the six typological classes shown in Table 2 are obtained, for which an ID is defined as a function of the category assigned to each parameter, TxRy, where letter T is associated to construction timespan (i.e., T1 for < 1919; T2 for 1919–1961; T3 for >1961); and letter R is associated to the state of repair (R1 for Excellent and Good—D0 and D1 < 1/3, and R2 for Mean and Poor—D1 > 1/3, D2–D4). Moreover, the relative frequency distribution of the census-based typological classes in the increased database is also presented in the last column of Table 2. The typological classes with the higher percentage of buildings are T1R1 (44.67%), T3R1 (20.81%), T2R1 (16.66%). Typological classes with state of repair R2 are always characterized by a lower percentage, with the maximum value equal to 10.08% for T1R2.

Table 2. Census building typological classification and relative frequency distribution of the increased database.

ID	Construction Timespan, T	State of Repair, R	Frequency Distribution [%]
T1R1	<1919	R1	44.67
T2R1	1919–1961	R1	16.66
T3R1	>1961	R1	20.81
T1R2	<1919	R2	10.08
T2R2	1919–1961	R2	3.47
T3R2	>1961	R2	4.31

4. Building Damage State

The building damage state needs to be defined for each item of the database to derive the damage fragility curves. The AeDES form indexes the damage occurred to different structural and non-structural elements, such as: vertical structures (index 1) and floor structures (2), stairs (3), roof (4), and partition walls (5). As already mentioned, the pre-existing damage (6) is also surveyed.

Starting from the collected AeDES damage, the building damage state *DS* was evaluated according to [28], with the following equation, based on the size of the structural elements and on costs of typical reparation techniques:

$$DS = \left| \frac{\sum_{i=1}^{5} d_i \, w_i \, S_i}{\sum_{i=1}^{5} w_i \, S_i} \right| - d_6 \quad (1)$$

where:

- d_i is the single-element damage associated with the damage grades and extensions collected with the AeDES form as shown in Table 3;

Table 3. Association of AEDES damage grades and extensions with structural element damage grade.

AeDES Form				Element Damage Grade
D0	**D1**	**D2–D3**	**D4–D5**	d_i
Null	**Light**	**Medium Severe**	**Very Heavy**	
✓				0
	<1/3			1
	1/3–2/3			1
	>2/3			1
		<1/3		2
	<1/3	<1/3		2
	1/3–2/3	<1/3		2
	>2/3	<1/3		2
	<1/3	1/3–2/3		3
		1/3–2/3		3
		>2/3		3
	<1/3	>2/3		3
			<1/3	4
	<1/3		<1/3	4
	1/3-2/3		<1/3	4
		<1/3	<1/3	4
	<1/3	<1/3	<1/3	4
		1/3–2/3	<1/3	5
		>2/3	<1/3	5
	<1/3		1/3–2/3	5
			1/3–2/3	5
	1/3–2/3		1/3–2/3	5
		<1/3	1/3–2/3	5
		1/3–2/3	1/3–2/3	5
			>2/3	5
	<1/3		>2/3	5
		<1/3	>2/3	5

- w_i is the weight assigned to each structural and non-structural element, defined as a function of the costs of typical reparation techniques and it assumes these values: $w_1 = 1.0$, $w_2 = w_3 = w_4 = 0.5$, and $w_5 = 0.3$ [28];
- S_i is the surface of the structural and non-structural elements.

In Figure 2, for each typological class defined in the previous section, the relative frequency distributions of damage state *DS* are shown in the histograms for the states of repair R1 and R2. Moreover, in the same figure, the cumulative damage trend is also reported. In Figure 2, the lowest damage states *DS*1 are the most populated for all typological classes, and the relative frequency distributions of buildings decrease in the highest damage state. Moreover, the cumulative damage curves underline a lower vulnerability of newer buildings, especially for the structures built after 1961 (T3). The state of repair parameter shows a trend sometimes counterintuitive, with a higher percentage of buildings in R1 than R2. This result is overturned if the data are further disaggregated, including the *PGA* intensity measure.

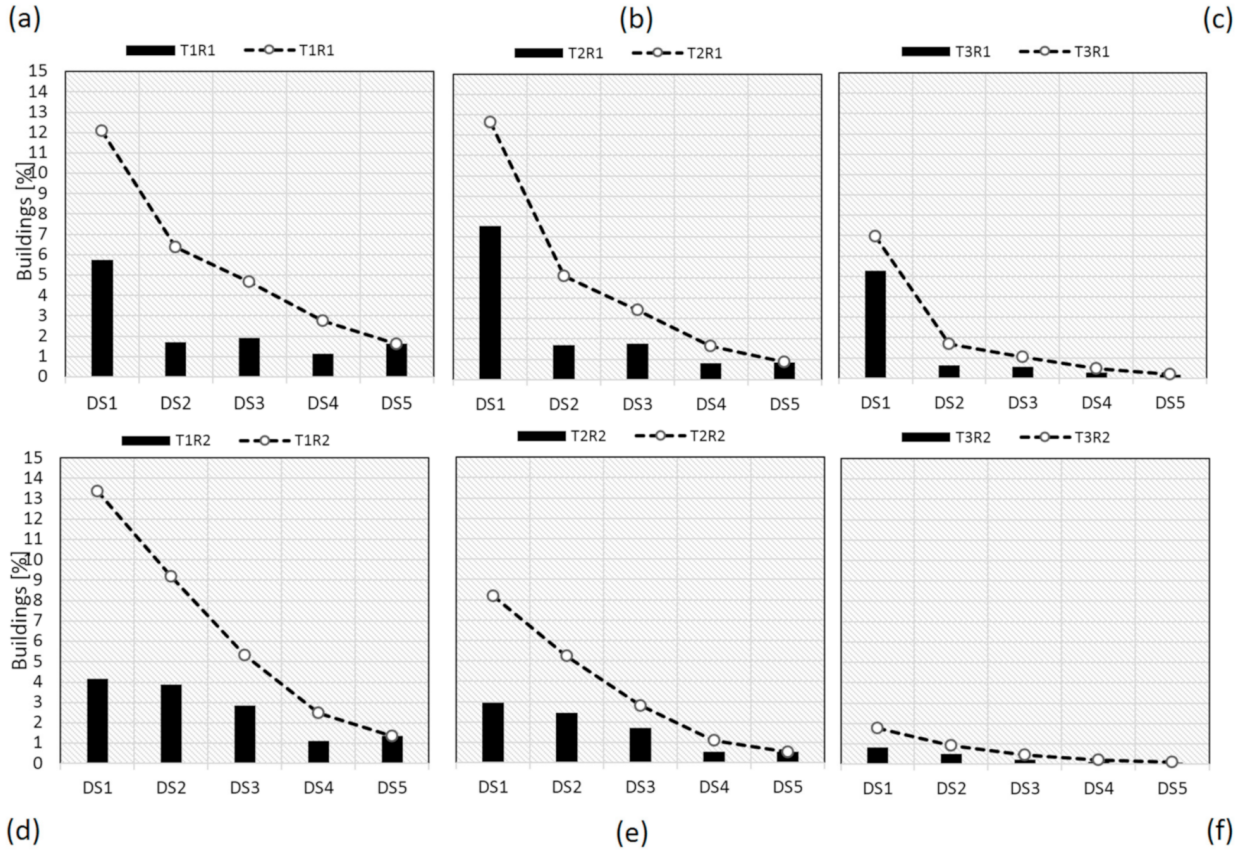

Figure 2. Relative frequency distribution of census-based typological classes for each damage: (**a**) T1R1, (**b**) T2R1, (**c**) T3R1, (**d**) T1R2, (**e**) T2R2, and (**f**) T3R2.

5. Damage Fragility Curves

5.1. Curves for Construction Timespan and State of Repair

The main aim of this work was to develop damage fragility curves according to the building damage state defined in the previous section, providing the probability of reaching or exceeding a specific building damage state.

Following other literature works on damage fragility curves [2,28,34,55], the log-normal function was used to fit the observed distribution of the surveyed damage points, according to the following equation:

$$P[DS \geq DS_i|PGA] = \Phi\left(\frac{\ln(PGA) - \mu}{\beta}\right) \quad (2)$$

where $P[DS \geq DS_i|PGA]$ is the probability of reaching or exceeding a specific damage state DS_i given a PGA value; $\Phi(\cdot)$ is the standard normal cumulative distribution function, μ is the logarithmic mean, and β is the logarithmic standard deviation.

The parameters μ and β were estimated with the maximum likelihood estimation method (e.g., [44,45]), assuming that the observed damage points follow the binomial distribution. Moreover, to avoid curves intersection for $PGA > 0.03$ g, the parameter β was constrained to be equal or increasing with higher damage states DS_i [56].

The completeness of the building data sample greatly influences the parameters of the fragility curves, with an increase of the exceedance probability, especially for low PGA values, as shown in Figure 3a for the T1R1 typological class. Uninspected buildings were included in the database to overcome this issue, considering both partially covered municipalities and municipalities entirely absent in the AeDES database (Figure 1), avoiding overestimating the exceedance probability for low PGA bins (Figure 3b). In Figure 3, and in

the following ones, continuous fragility curves are compared with discrete points observed after the 2009 L'Aquila earthquake. This comparison, and the general procedure for the derivation of fragility curves, serves as validation of the proposed analytical functions.

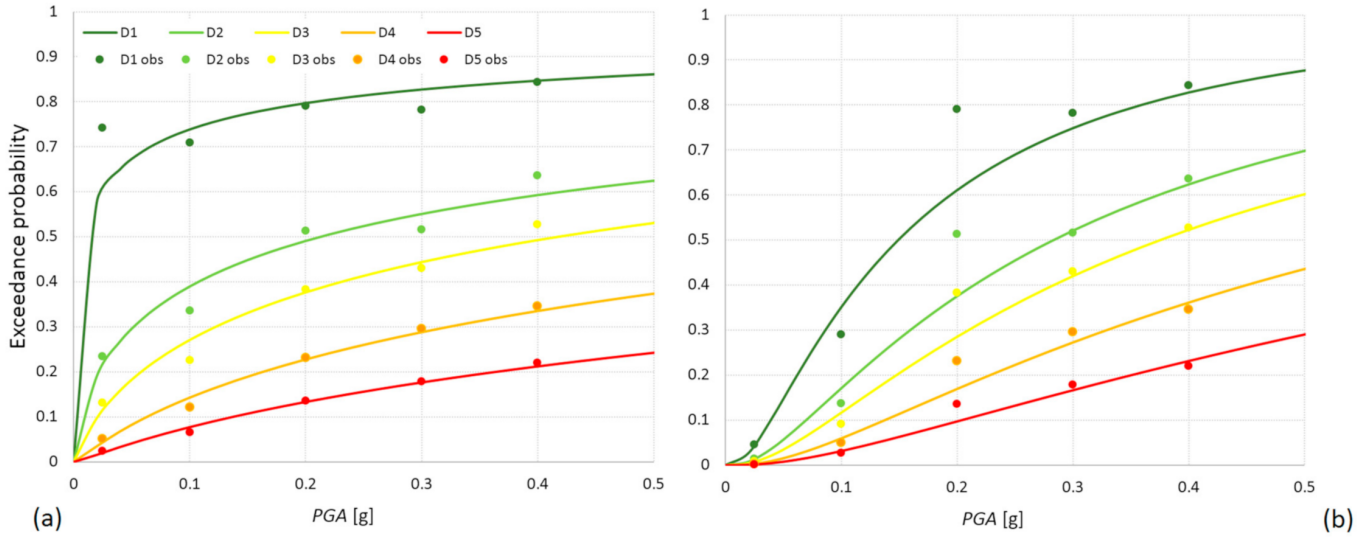

Figure 3. Damage fragility curves for typological class T1R1: discrete observed data and continuous fragility functions; (**a**) not accounting and (**b**) accounting for uninspected buildings.

In Figure 4, fragility curves fitting observed damage data for all typological classes are shown. As might be expected, older buildings are more vulnerable than newer ones leading to a higher exceedance probability for all damage states. This behavior is marked for both the states of repair R1 and R2 (Figure 4). Moreover, a higher vulnerability of buildings with state of repair R2 can be observed for all construction timespan classes. The same trend is confirmed in Table 4, where the median values $\theta = e^{\mu}$ (thus in units of g) of newer buildings are always greater than the older ones. Similarly, the typological classes with state of repair R2 always have lower median values with a consequent higher probability for given *PGA* value. Finally, an increasing median value can be observed with the increase of damage state. In Table 4, the median of PGAs, θ, is preferred to the mean of the natural logarithms of the PGAs, μ, since the numeric values of the former are easier to interpret. Logarithmic standard deviation, β, in Table 4 and in Figure 4 is smaller than in other similar works [2,34] and only Rosti et al. [29] present even smaller values resorting, however, to quality of masonry, stiffness of floors, presence of earthquake-resistant details, information that are not available in census.

Table 4. Parameters of log-normal fragility curves for the census-based typological classes accounting for construction timespan and state of repair.

	D1		D2		D3		D4		D5	
Typological Class	θ	β	θ	β	θ	β	θ	β	θ	β
	[g]	**[ln(g)]**	**[g]**	**[ln(g)]**	**[g]**	**[ln(g)]**	**[g]**	**[ln(g)]**	**[g]**	**[ln(g)]**
T1R1	0.149	1.042	0.283	1.094	0.375	1.109	0.603	1.152	0.987	1.230
T2R1	0.188	1.236	0.526	1.348	0.797	1.389	1.541	1.429	2.637	1.459
T3R1	0.447	1.388	2.113	1.578	3.104	1.578	5.571	1.578	16.143	1.777
T1R2	0.115	0.936	0.208	1.175	0.365	1.298	0.593	1.291	0.977	1.358
T2R2	0.181	1.113	0.359	1.348	0.787	1.542	1.531	1.529	2.627	1.562
T3R2	0.344	1.007	0.719	1.207	1.197	1.243	5.561	1.745	15.020	1.866

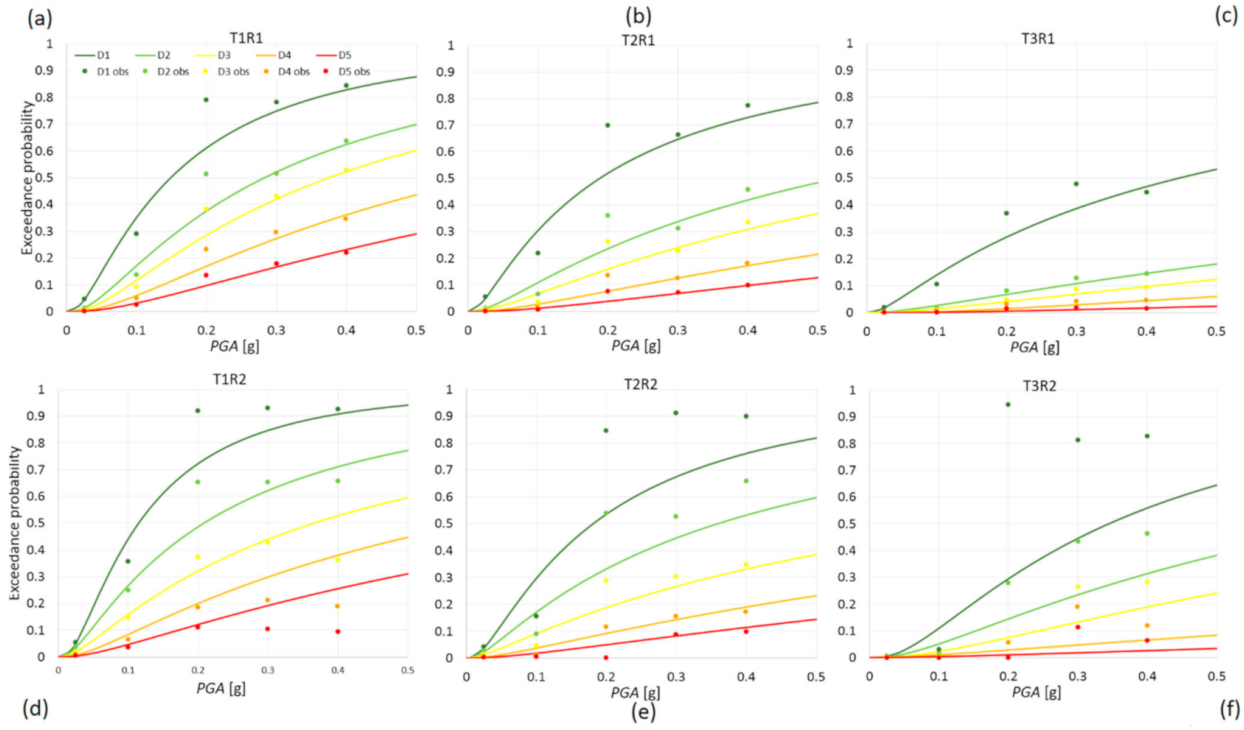

Figure 4. Fragility curves fitting the observed damage data for typological classes: (**a**) T1R1, (**b**) T2R1, (**c**) T3R1, (**d**) T1R2, (**e**) T2R2, and (**f**) T3R2.

5.2. Curves for Construction Timespan, State of Repair R1, and Number of Stories

In this section, further fragility curves are developed accounting also for the number of stories parameter. This parameter was considered only for buildings with state of repair R1. State of repair R2 constructions are not as frequent and when disaggregated according to number of stories become too few to get consistent results (i.e., taller buildings being more vulnerable while holding all other factors constant).

In particular, as shown in Table 5, six typological classes were defined, following the previous three construction timespan categories defined in Section 3 and introducing two categories for the number of stories above ground, namely one story and more than one story. In Table 5, the six categories are identified with an ID as a function of the category assigned to each parameter, TxRySz, similarly to what was defined in Section 3 where letter T is associated with construction timespan; letter R is associated with the state of repair (only R1 is considered); and letter S is associated with the number of stories (i.e, S1 for one story; S2 for more than one story). Overall, the buildings with state of repair R1 are more than 308,000; their relative frequency distribution is shown in the last column Table 5; it is possible to note that the buildings with more than one story are about the 84% of the total subset.

Table 5. Census building typological classification and relative frequency distribution accounting for construction timespan, state of repair R1, and number of stories.

ID	Construction Timespan, T	State of Repair, R	No. of Stories, S	Frequency Distribution [%]
T1R1S1	<1919	R1	1	8.36
T1R1S2	<1919	R1	>1	46.03
T2R1S1	1919–1961	R1	1	3.15
T2R1S2	1919–1961	R1	>1	17.13
T3R1S1	>1961	R1	1	4.36
T3R1S2	>1961	R1	>1	20.97

In Figure 5, it is possible to note a higher percentage of damaged buildings in typological classes with more than 1 story, as confirmed from the cumulative damage curves shown in the same figure. All other parameters being equal, taller buildings show higher vulnerability for all damage states Figure 6 and Table 6. The median values shown in Table 6 for the two number of stories categories of a single construction timespan always bracket the corresponding median value of the same construction timespan, and R1 state of repair category, in Table 4.

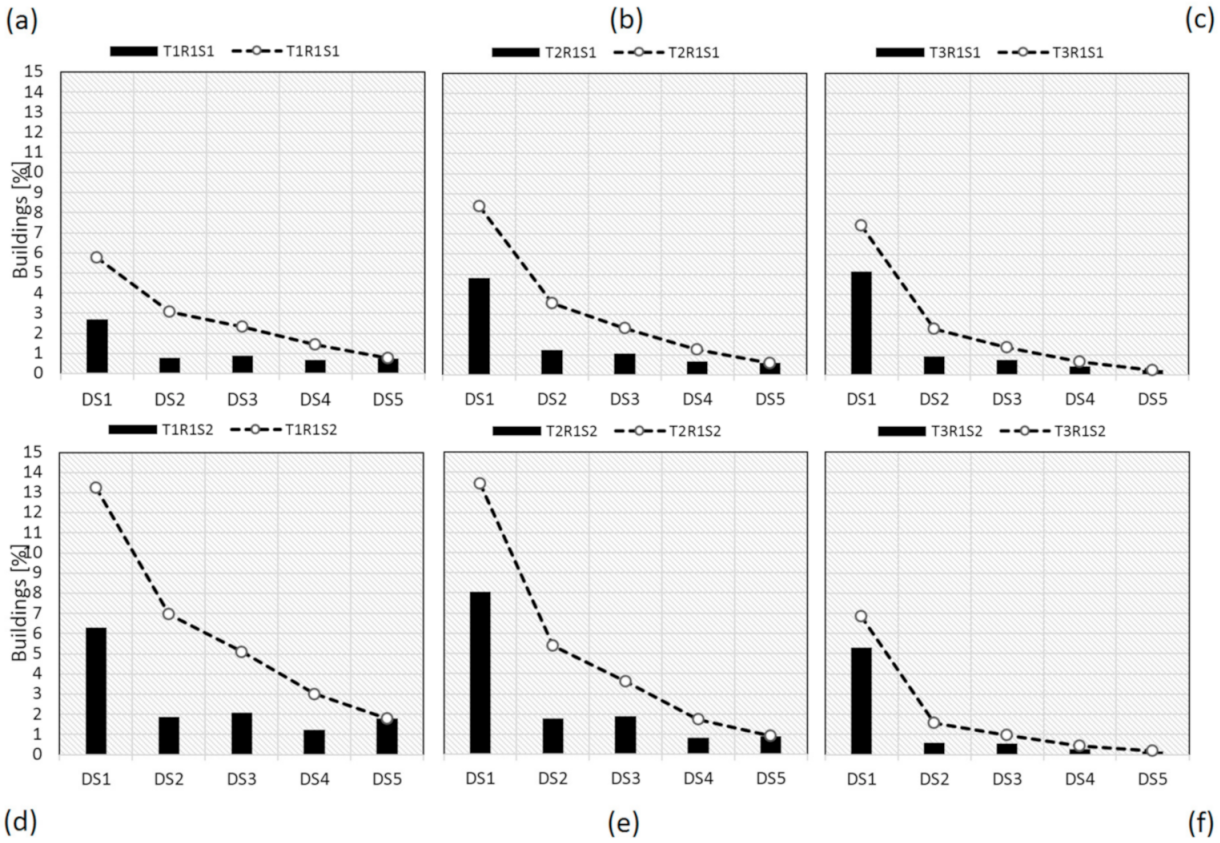

Figure 5. Relative frequency distribution of census-based typological classes for each damage state with state of repair R1: (**a**) T1R1S1, (**b**) T2R1S1, (**c**) T3R1S1, (**d**) T1R1S2, (**e**) T2R1S2, and (**f**) T3R1S3.

Table 6. Parameters of log-normal fragility curves for the census-based typological classes accounting for construction timespan, State of repair R1, and number of stories.

	D1		D2		D3		D4		D5	
Typological Class	θ	β	θ	β	θ	β	θ	β	θ	β
	[g]	[ln(g)]	[g]	[ln(g)]	[g]	[ln(g)]	[g]	[ln(g)]	[g]	[ln(g)]
T1R1S1	0.238	1.050	0.409	1.093	0.521	1.114	0.838	1.207	1.582	0.238
T1R1S2	0.140	1.039	0.271	1.096	0.362	1.111	0.584	1.150	0.950	0.140
T2R1S1	0.306	1.365	0.843	1.519	1.413	1.610	2.820	1.712	4.755	0.306
T2R1S2	0.175	1.215	0.495	1.327	0.744	1.362	1.423	1.389	2.449	0.175
T3R1S1	0.742	1.656	3.800	1.939	6.798	1.993	13.279	1.993	51.587	0.742
T3R1S2	0.392	1.319	1.808	1.486	2.602	1.486	4.590	1.486	12.295	0.392

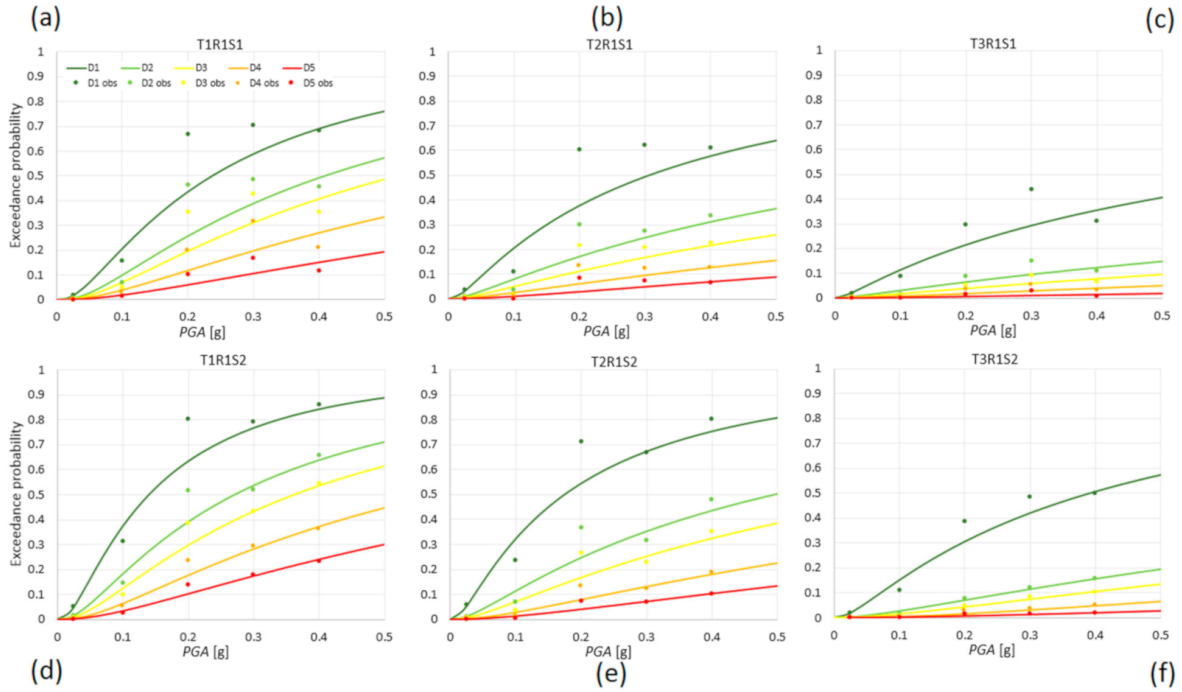

Figure 6. Fragility curves fitting observed damage data for typological classes with state of repair R1: (**a**) T1R1S1, (**b**) T2R1S1, (**c**) T3R1S1, (**d**) T1R1S2, (**e**) T2R1S2, and (**f**) T3R1S2.

6. Damage Risk Scenario in IRMA Platform

The damage fragility functions derived in the previous sections were used to develop damage risk maps for all the municipalities of Abruzzo region. The Italian Risk Maps (IRMA) information technology platform [15] was used to generate the maps. IRMA collects exposure data from the Italian census delivering, for each municipality, a disaggregation of residential buildings in terms of structural material, construction timespan, number of stories. IRMA also stores hazard data derived from the official national seismic hazard map [57], which is also used in the Italian building code [58]. Finally, this platform implements a percentage distribution of each municipality surface in the five soil categories of Eurocode 8 [59] according to the shear velocity values of the map developed by Mori et al. [60]

Whereas all these data are already loaded in the platform, the user needs to upload two key contributions: (i) an exposure-vulnerability association, and (ii) a set of fragility curves. The exposure-vulnerability association relates census categories to vulnerability classes. Buildings having the same features (e.g., being built before 1919 and being one story tall) can belong to just one vulnerability class or can be distributed between two (or more) vulnerability classes, according to user-defined percentages. In the present work, buildings belonging to a TxRy census class were distributed in two vulnerability classes based on percentage disaggregation of state of repair (Table 7), information not present in the current version of IRMA. For each vulnerability class, a set of five fragility functions needs to be described by the user in terms of θ and β. Standard deviation values can vary from a damage level to the others, but the platform does not accept entries involving curve intersection for 0.03 g < *PGA* < 1.00 g.

Once the upload process is complete, IRMA can develop damage risk maps for aggregated hazard for a specific return period (also known as conditional damage), for an observation time window (also known as unconditional damage), or for a scenario shakemap. Additionally, the platform can deliver risk maps in terms of unusable buildings, economic losses, human casualties based on several models [10,13,48,61]. In the following only damage risk maps for Abruzzo municipalities for a 50-year time window will be presented, but alternative uses of the platform are available in the literature [62,63].

Table 7. Simplified census classes TxSy, related to construction timespan (T) and number of stories (S), percentage disaggregation according to state of repair (R).

Simplified Census Class	R1	R2
	[%]	[%]
T1S1	80.86	19.14
T1S2	81.72	18.28
T2S1	81.36	18.64
T2S2	83.04	16.96
T3S1	82.08	17.92
T3S2	82.98	17.02

Damage risk maps are shown in Figure 7, wherein the percentage of URM buildings of each municipality with reached damage level DS is plotted. As expected, a systematic reduction of the percentages can be observed for increasing damage level (and hence, moving from a subplot to the next, a consequence of fragility curves not intersecting each other). Within a given subplot, percentages increase moving from the coast to the boundary with Lazio region, as a consequence of increasing seismic hazard. Nonetheless, exceptions within this trend can be observed, with individual municipalities presenting a darker or lighter tone compared to adjacent ones. These exceptions are thus related to a change in the vulnerability of the building portfolio, with the latter being comparatively older, taller, or in a worse state of repair. Given that the platform also delivers natural numbers of buildings, as well as building surfaces and not just percentages, maps such as those in Figure 7 can be used for allocating resources within risk mitigation policies. Moreover, simulations of such policies can be developed as well by modifying building fragility to decide between different options and to motivate stakeholders.

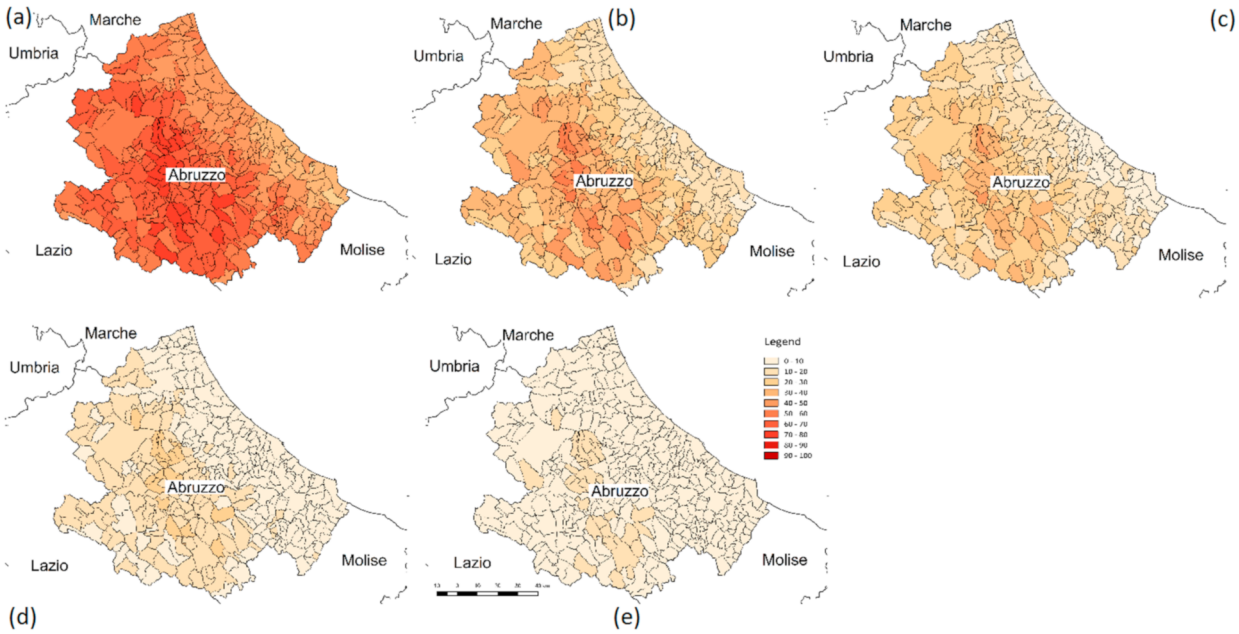

Figure 7. Abruzzo damage risk maps for an observation window of 50 years: (**a**) D1, (**b**) D2, (**c**) D3, (**d**) D4, (**e**) D5. Percentage of municipality URM buildings reaching corresponding damage level.

7. Conclusions

Earthquakes are responsible for most losses in Italy, considering both natural and man-induced hazards. Unreinforced masonry (URM) constructions are usually more vulnerable than reinforced concrete ones, and therefore they require special attention within risk analyses and mitigation policies. Such approaches require dealing with a

large number of buildings, hence making direct and detailed inspections unpractical. On the other hand, in Italy census surveyed residential buildings all over the national territory for decades. Consequently, there is a sheer interest in developing earthquake damage fragility curves for classes of buildings whose definition is based on parameters available in the census inventory. Therefore, six URM building classes, depending on three construction timespan categories and two state of repair categories available from the census, were defined and their fragility was evaluated resorting to data from the 2009 L'Aquila earthquake. Construction features and damage level for about 57,000 inspected buildings were complemented with data derived from census for about 308,000 buildings, not inspected since it is undamaged. A categorical value of the peak ground acceleration (*PGA*) was associated with each building based on the event shakemap published by the Italian National Institute of Geophysics and Volcanology. *PGA*-conditioned log-normal fragility curves were derived for five damage states of each of the defined six-building classes, maximizing likelihood. Older buildings are more vulnerable, but the state of repair is pivotal on earthquake fragility. Number of stories, a piece of information available in census, is less crucial and delivers consistent results (taller constructions being more vulnerable) only for those buildings presenting a better state of repair. Derived fragility curves allow implementing scenario and risk analyses in available on-line platforms, such as The Italian Risk Maps (IRMA) information technology platform. An application of the fragility curves to the Abruzzo region in Italy was developed to exemplify the potential of the proposed models for a 50-years observation time window (unconditional damage risk map). At the same time, IRMA exposure information does not retrieve from census data about state of repair, which was implemented only by means of an appropriate percentage distribution based on construction timespan. Therefore, it is recommended that future updates of IRMA account also for this piece of information.

Author Contributions: Conceptualization, M.Z. and L.S.; methodology, M.Z. and L.S.; validation, M.Z. and L.S.; formal analysis, M.Z.; data curation, M.Z.; writing—original draft preparation, M.Z. and L.S.; writing—review and editing, M.Z. and L.S.; visualization, M.Z.; project administration, L.S.; funding acquisition, L.S. All authors have read and agreed to the published version of the manuscript.

Funding: This work has been partially carried out under the program "Dipartimento di Protezione Civile—Consorzio RELUIS".

Institutional Review Board Statement: Not applicable.

Informed Consent Statement: Not applicable.

Data Availability Statement: The data supporting the findings of the article is available at: http://egeos.eucentre.it/danno_osservato/web/danno_osservato?lang=EN (accessed on 1 June 2021).

Acknowledgments: The authors wish to thank the Dipartimento di Protezione Civile for granting access to the damage and usability database of the L'Aquila earthquake. The opinions expressed in this publication are those of the authors and are not necessarily endorsed by the Dipartimento della Protezione Civile.

Conflicts of Interest: The authors declare no conflict of interest.

References

1. Rosti, A.; Rota, M.; Penna, A. Damage classification and derivation of damage probability matrices from L'Aquila (2009) post-earthquake survey data. *Bull. Earthq. Eng.* **2018**, *16*, 3687–3720. [CrossRef]
2. Del Gaudio, C.; De Martino, G.; Di Ludovico, M.; Manfredi, G.; Prota, A.; Ricci, P.; Verderame, G.M. Empirical fragility curves for masonry buildings after the 2009 L'Aquila, Italy, earthquake. *Bull. Earthq. Eng.* **2019**, *17*, 6301–6330. [CrossRef]
3. Shabani, A.; Kioumarsi, M.; Zucconi, M. State of the Art of Simplified Analytical Methods for Seismic Vulnerability Assessment of Unreinforced Masonry Buildings. *Eng. Struct.* **2021**, *239*, 112280. [CrossRef]
4. Şengezer, B.; Ansal, A. Probabilistic evaluation of observed earthquake damage data in Turkey. *Nat. Hazards* **2007**, *40*, 305–326. [CrossRef]
5. Romano, F.; Faggella, M.; Gigliotti, R.; Zucconi, M.; Ferracuti, B. Comparative seismic loss analysis of an existing infilled RC building based on element fragility functions proposals. *Eng. Struct.* **2018**, *177*, 707–723. [CrossRef]

6. Calvi, G.M. Choices and criteria for seismic strengthening. *J. Earthq. Eng.* **2013**, *17*, 769–802. [CrossRef]
7. Romano, F.; Alam, M.S.; Zucconi, M.; Faggella, M.; Barbosa, A.R.; Ferracuti, B. Seismic demand model class uncertainty in seismic loss analysis for a code-designed URM infilled RC frame building. *Bull. Earthq. Eng.* **2021**, *19*, 429–462. [CrossRef]
8. Ferracuti, B.; Savoia, M.; Zucconi, M. RC frame structures retrofitted by FRP-wrapping: A model for columns under axial loading and cyclic bending. *Eng. Struct.* **2020**, *207*, 110243. [CrossRef]
9. Dolce, M.; Speranza, E.; Bocchi, F.; Conte, C. Probabilistic assessment of structural operational efficiency in emergency limit conditions: The I.OPà.CLE method. *Bull. Earthq. Eng.* **2018**, *16*, 3791–3818. [CrossRef]
10. Di Ludovico, M.; Prota, A.; Moroni, C.; Manfredi, G.; Dolce, M. Reconstruction process of damaged residential buildings outside historical centres after the L'Aquila earthquake: Part I—"Light damage" reconstruction. *Bull. Earthq. Eng.* **2017**, *15*, 667–692. [CrossRef]
11. Polese, M.; Di Ludovico, M.; Prota, A. Post-earthquake reconstruction: A study on the factors influencing demolition decisions after 2009 L'Aquila earthquake. *Soil Dyn. Earthq. Eng.* **2018**, *105*, 139–149. [CrossRef]
12. Cosenza, E.; Del Vecchio, C.; Di Ludovico, M.; Dolce, M.; Moroni, C.; Prota, A.; Renzi, E. The Italian guidelines for seismic risk classification of constructions: Technical principles and validation. *Bull. Earthq. Eng.* **2018**, *16*, 5905–5935. [CrossRef]
13. Dolce, M.; Prota, A.; Borzi, B.; da Porto, F.; Lagomarsino, S.; Magenes, G.; Moroni, C.; Penna, A.; Polese, M.; Speranza, E.; et al. Seismic risk assessment of residential buildings in Italy. *Bull. Earthq. Eng.* **2021**, *19*, 2999–3032. [CrossRef]
14. Masi, A.; Lagomarsino, S.; Dolce, M.; Manfredi, V.; Ottonelli, D. Towards the Updated Italian Seismic Risk Assessment: Exposure and Vulnerability Modelling. *Bull. Earthq. Eng.* **2021**, *19*, 3253–3286. [CrossRef]
15. Borzi, B.; Onida, M.; Faravelli, M.; Polli, D.; Pagano, M.; Quaroni, D.; Cantoni, A.; Speranza, E.; Moroni, C. IRMA platform for the calculation of damages and risks of Italian residential buildings. *Bull. Earthq. Eng.* **2021**, *19*, 3033–3055. [CrossRef]
16. Dolce, M.; Speranza, E.; Giordano, F.; Borzi, B.; Bocchi, F.; Conte, C.; Meo, D.; Faravelli, M.; Pascale, V. Da.DO–A web-based tool for analyzing and comparing post-earthquake damage database relevant to national seismic events since 1976. In Proceedings of the XVII National Conference ANIDIS, Pistoia, Italy, 17–21 September 2017; pp. 348–357.
17. Dolce, M.; Speranza, E.; Giordano, F.; Borzi, B.; Bocchi, F.; Conte, C.; Meo, A.D.; Faravelli, M.; Pascale, V. Observed damage database of past italian earthquakes: The da.D.O. WebGIS. *Boll. Geofis. Teor. Appl.* **2019**, *60*, 141–164. [CrossRef]
18. Whitman, R.V.; Reed, J.W.; Hong, S.T. Earthquake Damage Probability Matrices. In Proceedings of the 5th World Conference on Earthquake Engineering, Rome, Italy, 25–29 June 1973; pp. 2531–2540.
19. Rota, M.; Penna, A.; Strobbia, C.; Magenes, G. Typological Seismic Risk Maps for Italy. *Earthq. Spectra* **2011**, *27*, 907–926. [CrossRef]
20. Del Gaudio, C.; De Martino, G.; Di Ludovico, M.; Manfredi, G.; Prota, A.; Ricci, P.; Verderame, G.M. Empirical fragility curves from damage data on RC buildings after the 2009 L'Aquila earthquake. *Bull. Earthq. Eng.* **2017**, *15*, 1425–1450. [CrossRef]
21. Romano, F.; Zucconi, M.; Ferracuti, B. Seismic fragility curves for RC buildings at territorial scale. In Proceedings of the COMPDYN 2019—7th ECCOMAS Thematic Conference on Computational Methods in Structural Dynamics and Earthquake Engineering; Crete, Greece, 24–26 June 2019.
22. Del Gaudio, C.; Di Ludovico, M.; Polese, M.; Manfredi, G.; Prota, A.; Ricci, P.; Verderame, G.M. Seismic Fragility for Italian RC Buildings Based on Damage Data of the Last 50 Years. *Bull. Earthq. Eng.* **2021**, *18*, 2023–2059. [CrossRef]
23. Zucconi, M.; Romano, F.; Ferracuti, B. Effect of Building Sample Selection on Seismic Fragility Curves for RC Buildings at Territorial Scale. In Proceedings of the COMPDYN 2021 8th ECCOMAS Thematic Conference on Computational Methods in Structural Dynamics and Earthquake Engineering, Athens, Greece, 27–30 June 2021.
24. Ferlito, R.; Guarascio, M.; Zucconi, M. Assessment of a vulnerability model against post-earthquake damage data: The case study of the historic city centre of L'Aquila in Italy. In Proceedings of the 9th World Conference on Earthquake Resistant Engineering Structures, A Coruna, Spain, 8–10 July 2013; WIT Transactions on the Built Environment; pp. 393–404.
25. Zucconi, M.; Sorrentino, L.; Ferlito, R. Principal component analysis for a seismic usability model of unreinforced masonry buildings. *Soil Dyn. Earthq. Eng.* **2017**, *96*, 64–75. [CrossRef]
26. Chieffo, N.; Clementi, F.; Formisano, A.; Lenci, S. Comparative fragility methods for seismic assessment of masonry buildings located in Muccia (Italy). *J. Build. Eng.* **2019**, *25*, 100813. [CrossRef]
27. Zucconi, M.; Ferlito, R.; Sorrentino, L. Validation and extension of a statistical usability model for unreinforced masonry buildings with different ground motion intensity measures. *Bull. Earthq. Eng.* **2020**, *18*, 767–795. [CrossRef]
28. Zucconi, M.; Ferlito, R.; Sorrentino, L. Typological Damage Fragility Curves for Unreinforced Masonry Buildings affected by the 2009 L'Aquila, Italy Earthquake. *Open Civ. Eng. J.* **2021**, *15*, 117–134. [CrossRef]
29. Rosti, A.; Rota, M.; Penna, A. Empirical fragility curves for Italian URM buildings. *Bull. Earthq. Eng.* **2021**, *19*, 3057–3076. [CrossRef]
30. Lagomarsino, S.; Cattari, S.; Ottonelli, D. The heuristic vulnerability model: Fragility curves for masonry buildings. *Bull. Earthq. Eng.* **2021**, *19*, 3129–3163. [CrossRef]
31. Lagomarsino, S.; Giovinazzi, S. Macroseismic and mechanical models for the vulnerability and damage assessment of current buildings. *Bull. Earthq. Eng.* **2006**, *4*, 415–443. [CrossRef]
32. Zuccaro, G.; Cacace, F. Seismic vulnerability assessment based on typological characteristics. The first level procedure "SAVE.". *Soil Dyn. Earthq. Eng.* **2015**, *69*, 262–269. [CrossRef]
33. Grünthal, G. *Cahiers du Centre Européen de Géodynamique et de Séismologie: Volume 15–European Macroseismic Scale 1998*; European Center for Geodynamics and Seismology: Luxembourg, 1998.

34. Rota, M.; Penna, A.; Strobbia, C.L. Processing Italian damage data to derive typological fragility curves. *Soil Dyn. Earthq. Eng.* **2008**, *28*, 933–947. [CrossRef]
35. Benedetti, D.; Petrini, V. Sulla vulnerabilita sismica di edifici in muratura: Un metodo di valutazione. A method for evaluating the seismic vulnerability of masonry buildings. *L'industria Delle Costr.* **1984**, *19*, 66–74.
36. Vicente, R.; Parodi, S.; Lagomarsino, S.; Varum, H.; Mendes Silva, J.A.R. Seismic vulnerability and risk assessment: Case study of the historic city centre of Coimbra, Portugal. *Bull. Earthq. Eng.* **2011**, *9*, 1067–1096. [CrossRef]
37. ISTAT. 15° Censimento della Popolazione e Delle Abitazioni 2011. Available online: https://www.istat.it/it/dati-analisi-e-prodotti/banche-dati (accessed on 1 June 2021).
38. Chaulagain, H.; Rodrigues, H.; Silva, V.; Spacone, E.; Varum, H. Earthquake loss estimation for the Kathmandu Valley. *Bull. Earthq. Eng.* **2016**, *14*, 59–88. [CrossRef]
39. Motamed, H.; Calderon, A.; Silva, V.; Costa, C. Development of a probabilistic earthquake loss model for Iran. *Bull. Earthq. Eng.* **2019**, *17*, 1795–1823. [CrossRef]
40. Goretti, A.; Di Pasquale, G. Building inspection and damage data for the 2002 Molise, Italy, earthquake. *Earthq. Spectra* **2004**, *20*, S167–S190. [CrossRef]
41. Dolce, M.; Speranza, E.; Giordano, F.; Borzi, B.; Bocchi, F.; Conte, C.; Meo, D.; Faravelli, M.; Pascale, V. O-Uno strumento per la consultazione e la comparazione del danno osservato relativo ai più significativi eventi sismici in Italia dal 1976. In Proceedings of the XXVII Convegno ANIDIS-L'Ingegneria Sismica in Italia, Pistoia, Italy, 17–21 September 2017; p. SG03.348-357.
42. Dolce, M.; Moroni, C.; Samela, C.; Marino, M.; Masi, A.; Vona, M. Una Procedura di Normalizzazione del Danno per la Valutazione degli Effetti di Amplificazione Locale. (in Italian). In Proceedings of the X Convegno ANIDIS-L'Ingegneria Sismica in Italia, Potenza-Matera, Italy, 9–13 September 2001.
43. De Martino, G.; Di Ludovico, M.; Prota, A.; Moroni, C.; Manfredi, G.; Dolce, M. Estimation of repair costs for RC and masonry residential buildings based on damage data collected by post-earthquake visual inspection. *Bull. Earthq. Eng.* **2017**, *15*, 1681–1706. [CrossRef]
44. Baker, J.W. Efficient Analytical Fragility Function Fitting Using Dynamic Structural Analysis. *Earthq. Spectra* **2015**, *31*, 579–599. [CrossRef]
45. Buratti, N.; Minghini, F.; Ongaretto, E.; Savoia, M.; Tullini, N. Empirical seismic fragility for the precast RC industrial buildings damaged by the 2012 Emilia (Italy) earthquakes. *Earthq. Eng. Struct. Dyn.* **2017**, *46*, 2317–2335. [CrossRef]
46. Stannard, M.; Galloway, B.; Brunsdon, D.; Wood, P.; Beattie, G.; McCarthy, S.; Toner, R.; Clark, A.; Nolan, J.; Stoecklein, A. *Field Guide: Rapid Post Disaster Building Usability Assessment-Earthquakes*; Ministry of Business, Innovation and Employment: Wellington, New Zealand, 2014.
47. Zucconi, M.; Ferlito, R.; Sorrentino, L. Simplified survey form of unreinforced masonry buildings calibrated on data from the 2009 L'Aquila earthquake. *Bull. Earthq. Eng.* **2018**, *16*, 2877–2911. [CrossRef]
48. Di Ludovico, M.; Prota, A.; Moroni, C.; Manfredi, G.; Dolce, M. Reconstruction process of damaged residential buildings outside historical centres after the L'Aquila earthquake: Part II—"Heavy damage" reconstruction. *Bull. Earthq. Eng.* **2017**, *15*, 693–729. [CrossRef]
49. Rossetto, T.; D'Ayala, D.; Gori, F.; Persio, R.; Han, J.; Novelli, V.; Wilkinson, S.M.; Alexander, D.; Hill, M.; Stephens, S.; et al. The value of multiple earthquake missions: The EEFIT L'Aquila earthquake experience. *Bull. Earthq. Eng.* **2014**, *12*, 277–305. [CrossRef]
50. Sisti, R.; Di Ludovico, M.; Borri, A.; Prota, A. Damage assessment and the effectiveness of prevention: The response of ordinary unreinforced masonry buildings in Norcia during the Central Italy 2016–2017 seismic sequence. *Bull. Earthq. Eng.* **2019**, *17*, 5609–5629. [CrossRef]
51. Zucconi, M.; Ferlito, R.; Sorrentino, L. Verification of a usability model for unreinforced masonry buildings with data from the 2002 Molise, Earthquake. In Proceedings of the 10th International Masonry Conference, IMC, Milan, Italy, 9–11 July 2018; pp. 680–688.
52. Baggio, C.; Bernardini, A.; Colozza, R.; Corazza, L.; Bella, M.D.; Pasquale, G.D.I.; Dolce, M.; Goretti, A.; Martinelli, A.; Orsini, G.; et al. Field Manual for Post-Earthquake Damage and Safety Assessment and Short Term Countermeasures (AeDES). In *JRC Scientific and Technical Reports*; Pinto, A., Taucer, F., Goretti, A., Rota, M., Eds.; Translation from Italian; EUR 22868 EN-2007; Office for Official Publications of the European Communities: Luxembourg, 2007; ISBN 1018-5593.
53. Michelini, A.; Faenza, L.; Lauciani, V.; Malagnini, L. Shakemap Implementation in Italy. *Seismol. Res. Lett.* **2008**, *79*, 688–697. [CrossRef]
54. Faenza, L.; Lauciani, V.; Michelini, A. Rapid determination of the shakemaps for the L'Aquila main shock: A critical analysis. *Boll. Geofis. Teor. Appl.* **2011**, *52*, 407–425. [CrossRef]
55. Rossetto, T.; Ioannou, I.; Grant, D.N. *Existing Empirical Fragility and Vulnerability Relationships: Compendium and Guide for Selection*; GEM Foundation: Kampala, Uganda, 2013.
56. Porter, K. *A Beginner 's Guide to Fragility, Vulnerability, and Risk*; University of Colorado: Boulder, CO, USA, 2020; Volume 16, ISBN 9780387938363.
57. Stucchi, M.; Meletti, C.; Montaldo, V.; Crowley, H.; Calvi, G.M.; Boschi, E. Seismic Hazard Assessment (2003–2009) for the Italian Building Code. *Bull. Seismol. Soc. Am.* **2011**, *101*, 1885–1911. [CrossRef]

58. DMIT Decreto del Ministro delle Infrastrutture e dei Trasporti 17 Gennaio 2018. Aggiornamento delle "Norme Tecniche per le Costruzioni". *Gazzetta Ufficiale della Repubblica Italiana*, 20 Febrary 2018; n. 42. Supplemento Ordinario n. 8. 2018 (Italian technical standard).
59. EC8-1. *Eurocode 8: Design of Structures for Earthquake Resistance-Part 1: General Rules, Seismic Actions and Rules for Buildings*; European Committee for Standardization: Brussels, Belgium, 2004; ISBN 5935522004.
60. Mori, F.; Mendicelli, A.; Moscatelli, M.; Romagnoli, G.; Peronace, E.; Naso, G. A new Vs30 map for Italy based on the seismic microzonation dataset. *Eng. Geol.* **2020**, *275*, 105745. [CrossRef]
61. National Department of Civil Protection. (NDCP, ed., 2018); National Risk Assessment: Overview of the Potential Major Disasters in Italy. Available online: http://www.protezionecivile.gov.it/documents/20182/823803/ (accessed on 1 June 2021).
62. da Porto, F.; Donà, M.; Rosti, A.; Rota, M.; Lagomarsino, S.; Cattari, S.; Borzi, B.; Onida, M.; De Gregorio, D.; Perelli, F.L.; et al. Comparative analysis of the fragility curves for Italian residential masonry and RC buildings. *Bull. Earthq. Eng.* **2021**, *19*, 3209–3252. [CrossRef]
63. Borzi, B.; Faravelli, M.; Di Meo, A. Application of the SP-BELA methodology to RC residential buildings in Italy to produce seismic risk maps for the national risk assessment. *Bull. Earthq. Eng.* **2021**, *19*, 3185–3208. [CrossRef]